

# Model of local dynamic interaction between a water basin and the atmosphere under conditions of surface roughness

V.A. Shlychkov

*Institute of Water and Ecological Problems, Siberian Branch of the Russian Academy of Sciences, Novosibirsk*

Received September 17, 2001

The paper presents a mathematical formulation of the problem on describing small-scale interaction of water basin and the atmosphere under conditions of moderate wind, with the detailed account of the vertical turbulent exchange near water-air interface. The surface exchange is calculated with the account of viscous-buffer films in both natural environments. Description of wind-induced roughness is based on solution of transfer equation for spectral density. The calculated values of the energy influx to waves and dissipation rates in the near-surface layers and at depth well agree with the observation data. A parameterization scheme is developed to describe the near-water layer above sea waves.

## Introduction

The simulation of small-scale near-surface interaction of the atmosphere and water basin is very difficult because of nonstationarity and irregularity of the shape of interface caused by traveling waves. Recently, different approaches have been developed to describe turbulence fields near rough water surface. A number of models is based on individual simulation of the system of periodic waves.<sup>1,2</sup> In other approaches, spectrally averaged characteristics of the layer of wave interaction are studied using hypotheses of aerodynamic resistance of moving underlying surface.<sup>3,4</sup> Some simpler models account for wind roughness in an integral form, by calculating the roughness parameter of sea surface using well known Charnok formula.<sup>4</sup>

An interesting theoretical model for calculating resistance of rough surface is described in Refs. 3 and 5. This approach is based on equations of motion and balance of turbulent energy in the presence of moving obstacles; in equations, the obstacles are described using additional terms associated with the resistance of obstacles and proportional to the square of relative velocity of the mean flux. The model is impractical, primarily because the relationship between the resistance parameters and statistical characteristics of the roughness must be determined in it.

The next section formulates the problem, in which the model from Refs. 3 and 5 is generalized to include an additional equation for wave energy balance. This removes from consideration the unknown empirical parameters and makes it possible, on the basis of analysis of the energy bonds in the system near-water atmospheric layer – wind waves – water basin, to obtain a local interaction model, closed in the internal parameter space.

## Statement of the problem

Let us consider motion of airflow over water surface covered with moving roughness waves. For

determining the vertical structure of solution domain we will use the notion of a transient layer occupied by moving waves (see Ref. 4), and assume that the level  $z = 0$  coincides with the layer bottom (level of the mean position of wave troughs). We introduce the following notation:  $h_{10}$  is the top height of near-water layer; and  $h_s$  is the thickness of the transient layer. In the layer  $0 - h_s$ , there occurs a momentum exchange between the atmospheric airflow and waves due to normal pressure forces, as well as a transfer of tangential tensions to drifting current. It is assumed that the lower boundary of the region in water  $\tilde{H}$  is located at depth making no contribution to natural decay of the surface processes.

Assuming that the level  $h_{10}$  is located above the layer of wave interaction, for quasi-stationary conditions the dynamic equation is written as<sup>5</sup>:

$$\begin{aligned} \frac{\partial}{\partial z} K \frac{\partial U}{\partial z} &= \gamma_L |U - C| (U - C), \\ \frac{\partial}{\partial z} K \frac{\partial b}{\partial z} + KJ + \gamma_L |U - C|^3 - \varepsilon &= 0, \\ \frac{\partial}{\partial z} K \frac{\partial \varepsilon}{\partial z} + c_2 \frac{\varepsilon}{b} (KJ + \gamma_L |U - C|^3) - c_3 \frac{\varepsilon^2}{b} &= 0, \\ K &= c_1 \frac{b^2}{\varepsilon}, \end{aligned} \quad (1)$$

where  $U$  is the wind speed;  $b$  is the kinetic turbulence energy (KTE);  $\varepsilon$  is the rate of KTE dissipation;  $J = U_z^2 - \lambda \Theta_z$ ,  $\lambda$  is the buoyancy parameter,  $\Theta$  is the air temperature;  $C$  is the phase speed of waves;  $\gamma_L$  is the dimension parameter (in  $\text{m}^{-1}$ ) having the meaning of friction coefficient; and  $c_1$ ,  $c_2$ , and  $c_3$  are universal constants. It is assumed that  $\gamma_L$  vanishes above the level  $h_s$ .

For  $\tilde{H} < z < 0$ , the current in the water basin is described by the equations

$$\frac{\partial \tilde{U}}{\partial t} = \frac{\partial}{\partial z} \tilde{K} \frac{\partial \tilde{U}}{\partial z}, \frac{\partial \tilde{b}}{\partial t} = \frac{\partial}{\partial z} \tilde{K} \frac{\partial \tilde{b}}{\partial z} + \tilde{K} \tilde{J} - \tilde{\varepsilon},$$

$$\frac{\partial \tilde{\varepsilon}}{\partial t} = \frac{\partial}{\partial z} \tilde{K} \frac{\partial \tilde{\varepsilon}}{\partial z} + \tilde{c}_2 \frac{\tilde{\varepsilon}}{\tilde{b}} \tilde{K} \tilde{J} - \tilde{c}_3 \frac{\tilde{\varepsilon}^2}{\tilde{b}} = 0, \tilde{K} = \tilde{c}_1 \frac{\tilde{b}^2}{\tilde{\varepsilon}}, \quad (2)$$

where  $\tilde{J} = \tilde{U}_z^2 - g\beta_T T_z$ ;  $T(z)$  is the temperature of water;  $\beta_T$  is the thermal expansion coefficient of water;  $g$  is acceleration of gravity; and the tilde over the quantities indicates the water medium. The parameters of surface waves will be calculated using wave energy balance equation in the spectral representation<sup>6</sup>

$$\frac{\partial S}{\partial t} + C_x \frac{\partial S}{\partial x} + C_y \frac{\partial S}{\partial y} = I - D, \quad (3)$$

where  $S(\omega, \varphi, x, y, t)$  is the spectral density of wave energy,  $\omega$  is the frequency,  $\varphi$  is the direction of wave propagation;  $C_x, C_y$  are the component vectors of the group velocity along the directions  $x, y$ ;  $I$  is the wave energy supplied by wind; and  $D$  is the rate of energy dissipation due to wave disruption. Solution of equation (3) makes it possible to determine the mean roughness parameters. In particular, for elevation  $\sigma$  and thickness  $h_s$  we obtain<sup>4</sup>

$$\sigma^2 = \int_0^\infty \int_0^{2\pi} S d\omega d\varphi; \quad h_s = \sqrt{2\pi} \sigma. \quad (4)$$

Now we consider the boundary conditions. At the top boundary, the wind speed  $U_{10}$  is assumed to be

$$U = U_{10}; \quad \frac{\partial b}{\partial z} = 0; \quad K \frac{\partial \varepsilon}{\partial z} = -\kappa u_* \varepsilon \text{ for } z = h_{10}, \quad (5)$$

where  $u_*$  is the dynamic speed. In specifying conditions at water-air interface, KTE continuity at the surface, as in Ref. 2, is assumed

$$\tilde{U} = U, \quad \tilde{\rho} \tilde{b} = \rho b, \quad K = \nu, \quad \tilde{\rho} \tilde{K} \frac{\partial \tilde{U}}{\partial z} = \rho K \frac{\partial U}{\partial z},$$

$$\tilde{\rho} \tilde{K} \frac{\partial \tilde{b}}{\partial z} = \rho K \frac{\partial b}{\partial z} + \tilde{\rho} D_1, \quad \tilde{K} = l_0 \sqrt{\tilde{b}} \text{ for } z = 0, \quad (6)$$

where  $D_1 = 0.5g(1 - a) \int_0^\infty \int_0^{2\pi} D d\omega d\varphi$  is the KTE flux

into the water;  $\nu$  is the molecular viscosity of air; and parameter  $a < 1$  characterizes the fraction of wave energy converted to heat immediately above water surface and omitted within the model. The last condition in the system (6) determines the turbulent regime of the surface layer by specifying the scale length  $l_0$  associated with the intensity of roughness.

For the bottom boundary in the water we specify the conditions:

$$\tilde{U} = 0, \quad \frac{\partial \tilde{b}}{\partial z} = 0, \quad \frac{\partial \tilde{\varepsilon}}{\partial z} = 0 \text{ for } z = \tilde{H}. \quad (7)$$

By orienting the  $x$ -axis normal to the shore, we write the boundary condition for equation (3), along the shore, assuming statistical homogeneity of roughness with respect to  $y$

$$S = 0 \text{ for } x = 0. \quad (8)$$

As the initial conditions for equations (2) and (3), we specify the state of rest.

From analysis of energy relations for systems (1)–(3), it can be shown that the boundary conditions formulated above do not contradict the laws of energy conservation in the components of the natural system near-water layer – wind-induced waves – top layer of water basin. The necessary condition of the energy balance is given by the equation

$$0.5\tilde{\rho}g \int_0^\infty \int_0^{2\pi} I d\omega d\varphi = \rho\gamma_L \int_0^{h_s} C |U - C| (U - C) dz,$$

which provides closure for the problem with respect to the quantity  $\gamma_L$ , usually specified as an external parameter.

### Treatment of the viscous layers

Equations (1) are valid for developed turbulent regimes and fail for conditions realized near interface, where the turbulent viscosity is comparable to the molecular viscosity. The dependence  $K(z)$  in the viscous buffer air layer  $0 < z < h_v$  is approximated by the empirical formula<sup>5</sup>

$$K_v = \nu[(1 + 0.1\nu_* z/\nu)^2], \quad (9)$$

where  $\nu_*$  is dynamic speed of tangential friction; and the subscript  $\nu$  stands for viscous buffer layer. The layer thickness  $h_v$  is  $(30 - 50)\nu/\nu_*$ , in conformity with numerous estimates.<sup>3,5</sup>

For calculation of  $\nu_*$ , we use the equation of momentum conservation in the layer of moving obstacles

$$\rho u_*^2 = \rho\gamma_L \int_0^{h_s} |U - C| (U - C) dz + \rho\nu_*^2, \quad (10)$$

where the first term in the right-hand side describes the resistance to airflow due to obstacle shape; while overall, the equation characterizes the momentum loss due to Reynolds tensions counteracting the resistance forces.

Within the viscous buffer layer, it is assumed that

$$K_v \frac{\partial U}{\partial z} = \nu_*^2, \quad K_v \frac{\partial b}{\partial z} = \text{const},$$

which, combined with (9), makes it possible to reconstruct the velocity and KTE profiles as functions of  $z$  in this layer.

The viscous buffer layer in water is simulated by hypothesizing that the structure of near-wall turbulence in water and air is the same,<sup>5,7</sup> i.e., by assuming that

the distribution  $\tilde{K}(z)$  in formula (8) does not depend on whether parameters for water or air are used.

To calculate  $D_1$  in (6), the underwater dissipation determined by the parameter  $a$  must be known. Presently, the data on the rate of KTE influx into the water during wave overturning are very scarce. Here we only mention an estimate by Kitaigorodskii<sup>4</sup> ( $a = O(1)$ , consistent with measurements) and let  $a = 0.96$ . As numerical experiments show, such a value of  $a$  in water favors the formation of wind-driven mixing layer in which the calculated dissipation rate reasonably agrees with the observed  $\tilde{\epsilon}$  values.<sup>1,5</sup>

### Parameterization of the transient layer

We now will consider a numerical solution to the problem for conditions when roughness parameters vary little with time. Figure 1a presents KTE profiles in the near-water layer calculated assuming  $U_{10} = 8$  m/s for fetches  $x = 1-3, 5, 10, 20$  km (the curves are shifted in horizontal, and curve numbers correspond to distance from coast). The horizontal bar on the curves indicates the calculated height of the transition layer  $h_s$ . The vertical bar indicates the equilibrium  $b$  value, characteristic of the traditional layer of constant fluxes over non-moving underlying surface. The deviation of KTE profile from a constant level is explained by the resistance to the shape. From Fig. 1a it is seen that the deviation grows with increasing  $x$ , probably because the larger the fetch, the greater the height and length of the wind-induced waves.

The character of this KTE distribution, with a maximum near the level of wave crests and decay of induced perturbations at heights comparable with height of waves, is consistent with the turbulent characteristics on near-water layer described qualitatively in Ref. 3.

The vertical structure of KTE, in dimensionless coordinate  $\zeta$

$$\zeta = \int_0^{\zeta} dz/K \left( \int_0^h dz/K \right)^{-1}, \quad (11)$$

is presented in Fig. 1b (curves 1 and 2). The difference in the profiles is due to different boundary conditions at the bottom boundary; in the first case, initial conditions (6) were specified with a direct KTE tailoring at the surface  $z = 0$ . The input of turbulent energy to water in the course of wave disruption leads to large  $\tilde{b}$  values, an order of magnitude larger than KTE scale due to generation by shear. Since KTE values for water and air are required to coincide,  $b$  also has large values, leading to the fact that the profile peaks at the lower boundary (curve 1 in Fig. 1b) and KTE flux is directed from water to air. This effect, reminiscent of reflection of turbulent energy from the surface, manifest itself only in the lower centimeter-thick air layer; though it was not recorded in the field. Quite possibly, this is

due to the transfer of KTE from waves to air (such as during ripple); though this is not confirmed experimentally yet.

Therefore, we will not require KTE continuity at the interface and, instead of the system (6), consider the conditions

$$\rho K \frac{\partial b}{\partial z} = 0, \quad \tilde{\rho} \tilde{K} \frac{\partial \tilde{b}}{\partial z} = \tilde{\rho} D_1, \quad (12)$$

which again ensures balance of turbulent fluxes. Curve 2 in Fig. 1b is obtained by integration of the problem with the boundary conditions (12). We see that formulas (12) are a less restricted condition and provide physically more meaningful solution. Actually, the gradients of  $b$  near the surface are not high, the reflection effect is absent, and turbulent energy flux is directed toward water.

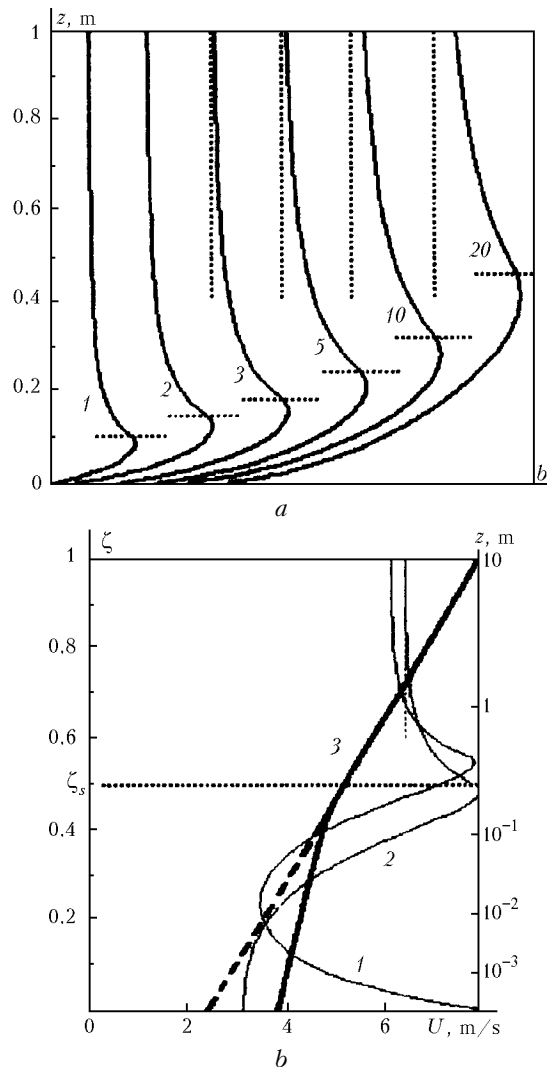


**Fig. 1.** (a) Profiles  $b(z)$  of the established turbulent regime in the near-water air layer (figures near curves correspond to the fetch in km); and (b) profiles of  $b$  calculated for boundary conditions (6) (curve 1) and (12) (curve 2), as well as the profile of  $U$  (curve 3) in dimensionless coordinate  $\zeta$ .

The deviation of wind speed from logarithmic profile over sea waves was discussed extensively in the literature.<sup>3,4</sup> Using field data, it was shown that the distortion of wind profile is observed only in the lowest air layer, most probably due to a change of turbulence fields under the influence of momentum flux directed toward waves. The reduction of resistance force due to the wave propagation velocity leads to an increase in the wave velocity near the wave crests by as much as 0.5–1 m/s under marine conditions. This velocity increase has the same order of magnitude as model-calculated values shown in Fig. 1b by solid line (curve 3). The logarithmically distributed  $U(z)$  becomes a linear function in  $\zeta$  coordinate; in Fig. 1b it is shown by dashed line (curve 3). The velocity profile has an inflection point, indicating the presence of thin transient layer. Outside this layer, the velocity follows almost linear law with the slopes  $u_*^2$  and  $v_*^2$  above and below the level  $\zeta = \zeta_s$ , respectively. Such a relationship is found in all calculations over a wide range of parameters. This provides a basis for construction of a simple parameterization of the transient layer. Approximating  $U(\zeta)$  by a piecewise linear function with a sewing at the inflection point, from the boundary conditions and momentum conservation equation (10) we obtain a system of nonlinear equations relating  $u_*$  and  $v_*$ . This system of equations is solved by iterations.

Comparison of this parameterization with logarithmic law has made it possible to calculate the roughness parameter  $z_0$  as a level, at which the velocity formally turns to zero. Presently, there are many empirical formulas for calculation of  $z_0$ , and most of them are inferred from observations in open sea with the developed roughness. These formulas can be useless for inland water basins because they have limited water area (fetch) and small value of the parameter  $C/u_*$ , which characterizes the “age” of the waves.<sup>3</sup> This is illustrated by Fig. 2 which shows the calculated  $z_0$  values as functions of wind speed for different distances from leeward coast (curves 1–3 are calculated for  $x = 5, 10,$  and  $20$  km). Also shown are distribution of roughness parameter, obtained by the method from Ref. 8 (curve 4) and using empirical Charnok formula<sup>4</sup>:

$$z_0 = mu_*^2/g, \quad (13)$$

with most frequently used values of the parameter  $m = 0.035$  and  $0.074$  (curves 5 and 6, respectively). Use of formula (13), as usual, for the ocean gives a monotonic increase of the roughness parameter with increasing wind speed; whereas its use for a limited fetch does not lead to such a dependence. For instance,  $z_0$  grows slower starting from  $U_h = 6$  m/s, practically leveling off at  $U_h = 8$  m/s (Fig. 2, curve 1), probably since the waves reach their limiting height at small distances from the coast. As the fetch increases (curves 2 and 3), the energy “saturation” of waves occurs at a larger wind speed until, in the limit as  $x \rightarrow \infty$ , the

Charnok formula becomes valid. The increase of  $z_0$  in the range  $U_h < 2$  m/s (curves 1 and 4) is due to the increase of the role of molecular sublayer in the regime of weak winds.

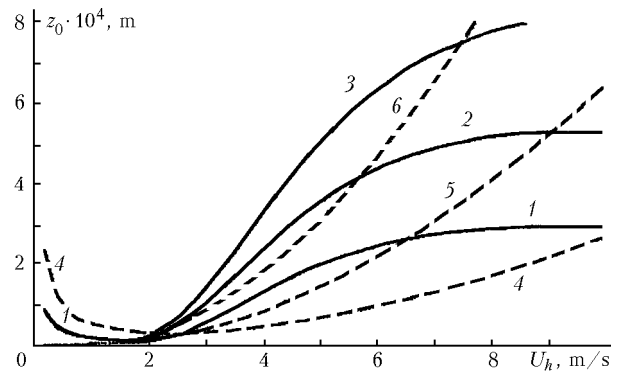


Fig. 2. Dependence of roughness parameter on wind speed for the fetches  $x = 5, 10,$  and  $20$  km (curves 1–3); dashed lines show empirical dependences (curves 4–6).

The model validation was made using data<sup>9</sup> obtained as part of the field experiment at reservoir of Wellington, Australia. The data describe the evolution of mixing layer in water under impact of wind-induced and shear turbulence during typical late-summer day. The sea breeze, with a maximum speed of 6.5 m/s, developed in the second half of the day, and weakened by the evening. The mean calculated height of the roughness was as large as 0.17 m for the fetch of 3 km (in specifying the fetch, the wind direction relative to coastal line and the position of the site on the reservoir were taken into account). Figure 3 shows the time variations of the model friction velocity in water and actual  $\tilde{u}_*$  values as given in Ref. 9 in the form of look-up tables. We note that the experimental values and theoretical curve quantitatively agree. Also good agreement is obtained for the dynamics of mixing layer and absolute values of the drift velocity.

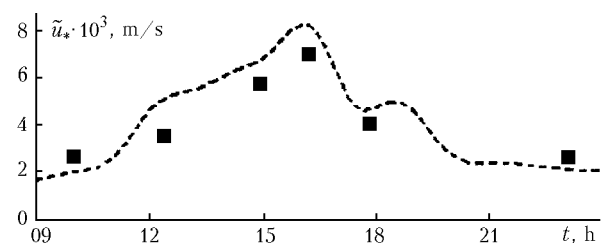


Fig. 3. Comparison of calculated (dashed) and actual (squares)  $\tilde{u}_*$  values.

## References

1. O.M. Phyllips, *Dynamics of the Upper Layer of Ocean* (Gidrometeoizdat, Leningrad, 1980), 319 pp.

2. V.D. Chalikov, *Mathematical Simulation of Wind-Induced Roughness* (Gidrometeoizdat, Leningrad, 1980), 48 pp.
3. R.S. Bortkovskii, E.K. Byutner, and S.P. Malevskii-Malevitch, *Transport Processes Near the Ocean-Atmosphere Interface* (Gidrometeoizdat, Leningrad, 1974), 239 pp.
4. S.A. Kitaigorodskii, *Physics of the Atmosphere - Ocean Interaction* (Gidrometeoizdat, Leningrad, 1970), 290 pp.
5. E.K. Byutner, *Dynamics of the Near-Water Air Layer* (Gidrometeoizdat, Leningrad, 1978), 158 pp.
6. I.V. Lavrenov, *Mathematical Simulation of Wind-Induced Roughness in Spatially Inhomogeneous Ocean* (Gidrometeoizdat, St.Petersburg, 1998), 499 pp.
7. S.A. Kitaigorodskii, *Izv. Akad. Nauk SSSR, Ser. Fiz. Atmos. Okeana* **33**, No. 6, 828-836 (1997).
8. V.N. Lykosov, *Vychislitel'nye Protsessy i Sistemy* (Nauka, Moscow), Issue 10, 65-95 (1993).
9. J. Imberger, *Limnol. Oceanogr.*, 30(4), 737-770 (1985).